



# Automatic Material Classification Using Thermal Finger Impression

Jacob Gately<sup>1</sup>, Ying Liang<sup>2</sup>, Matthew Kolessar Wright<sup>1</sup>,  
Natasha Kholgade Banerjee<sup>1</sup>, Sean Banerjee<sup>1</sup>, and Soumyabrata Dey<sup>1</sup>(✉)

<sup>1</sup> Clarkson University, 8 Clarkson Avenue, Potsdam, NY 13699, USA  
{gatelyjm,kolessmj,nbanerje,sbanerje,sdey}@clarkson.edu

<sup>2</sup> Cornell University, Ithaca, NY 14850, USA  
y12864@cornell.edu

**Abstract.** Natural surfaces offer the opportunity to provide augmented reality interactions in everyday environments without the use of cumbersome body-mounted equipment. One of the key techniques of detecting user interactions with natural surfaces is the use of thermal imaging that captures the transmitted body heat onto the surface. A major challenge of these systems is detecting user swipe pressure on different material surfaces with high accuracy. This is because the amount of transferred heat from the user body to a natural surface depends on the thermal property of the material. If the surface material type is known, these systems can use a material-specific pressure classifier to improve the detection accuracy. In this work, we address to solve this problem as we propose a novel approach that can detect material type from a user's thermal finger impression on a surface. Our technique requires the user to touch a surface with a finger for 2 s. The recorded heat dissipation time series of the thermal finger impression is then analyzed in a classification framework for material identification. We studied the interaction of 15 users on 7 different material types, and our algorithm is able to achieve 74.65% material classification accuracy on the test data in a user-independent manner.

**Keywords:** Multimaterial classification · Thermal imaging · Natural surface interface · Time series

## 1 Introduction

Sensor modalities outside the visible light domain such as depth, hyperspectral, and thermal cameras have begun to permeate the consumer space, and their ubiquity enables the spread of novel applications in the consumer domain. One such application is the use of any natural surface as a touchscreen interface to communicate with computing devices. While traditionally natural surface interaction has been performed in the color domain [1–3], a number of approaches [4–8] have demonstrated the effectiveness of using thermal sensors to perform natural surface interaction. Some of these works [6, 8] attempted to detect swipe

pressure because this can add a new dimension to the vocabulary space of swipe and gesture actions. For example, the same swipe pattern with different pressure can carry different meanings for the interacting computing device. One of the main challenges of this task is the manifestation of swipe pressure as heat signature varies with different surface materials. This is because the amount of heat transferred from the user body to a surface depends on the thermal property of the surface material. For example, swipe actions with similar pressure on concrete and wood surfaces would appear differently while recorded using a thermal camera. On the other hand, a hard swipe on a concrete surface can look similar to a soft swipe on a wood surface. Figure 1 illustrate the problem with an example. As a result, pressure detection accuracy suffers a great deal while performed across different materials. Our work aims to solve this problem with automatic material detection which should precede the swipe pressure classification. Once the surface material is identified using our method, a material-specific classifier can be applied to detect the swipe pressure.

To perform automatic material classification using thermal images, we proposed a novel approach where a user needs to touch the surface of a material for 2s with his finger. The thermal finger impression left on the surface is then tracked for 50s. The time series of decaying heat signature of the thermal finger impression is used in a random forest based classification framework to detect the surface material. The algorithm is tested on data captured from 15 different users interacting with 7 different material types including blackboard, polyester fabric, cotton cloth, concrete, drywall, laminate, and wood. The classification accuracy achieved on the test data set is 52% compared to the random guess probability of 14.29%. Further investigation suggests that thermal signature decay patterns of blackboard and concrete are almost similar. Similar behavior observed for thermal patterns of drywall, laminate, and wood. See Fig. 3 for details. This suggests us to cluster 7 material types into 4 classes (Class 1 - blackboard and concrete, class 2 - polyester fabric, class 3 - cotton cloth, class 4 - drywall, laminate, and wood) based on their thermal impressions. Since the appearance of swipe pressure in the thermal domain depends on the amount of heat transferred onto the surface and its decay pattern, we concluded that swipes with similar pressure would display a similar thermal signature on materials of each of these four classes. The classification accuracy achieved for the detection of 4 material classes is 74.65%. Compared to the probability of random guess (25%) this is a significant improvement.

The main contribution of this paper is a novel user-independent material detection method. We selected 7 different material types that commonly found in indoor scenarios, and we demonstrated that they can be divided into 4 clusters based on their thermal behaviors. The method should assist in improving the accuracy of the systems which aim to perform user swipe pressure classification on different material surfaces. This can be achieved by first detecting the thermal class of a material, and then using a pressure classifier specific to the thermal property of the material.

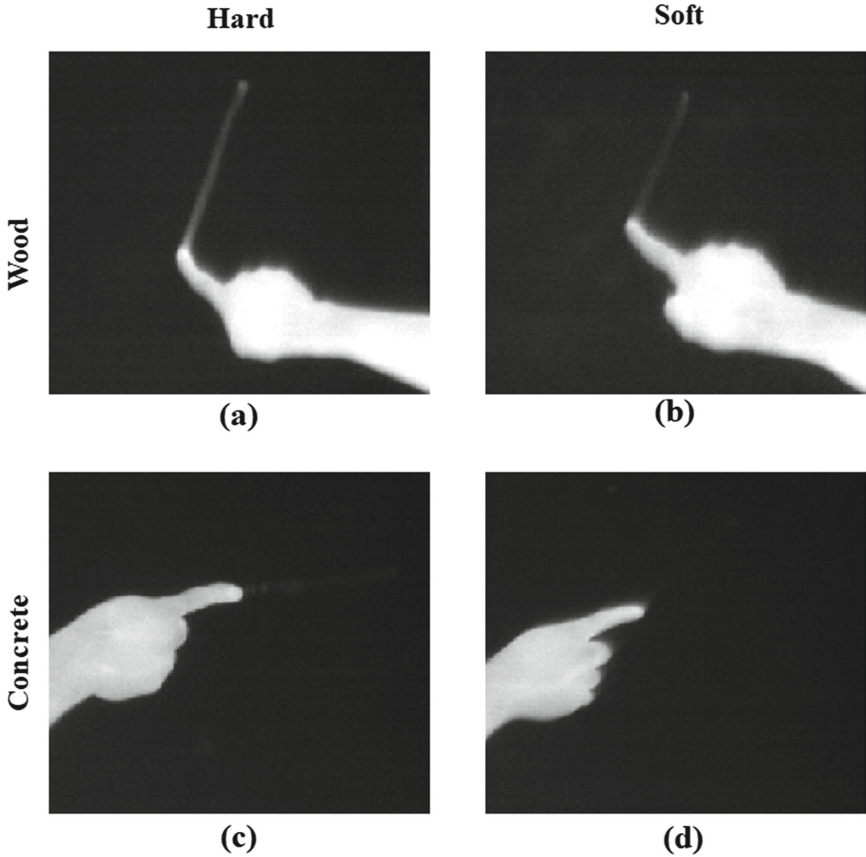


**Fig. 1.** This example illustrates how swipes with similar pressure can appear very different on different materials. (a) Hard swipe on wood, (b) soft swipe on wood, (c) hard swipe on concrete, (d) soft swipe on concrete.

## 2 Related Work

There have been several approaches that attempt to solve the problem of interaction with projected content on natural surfaces. While some of the work [1–3] used color cameras to detect user actions and gestures, others [4–8] leveraged on thermal domain data to address the problem. Few of the work [6–8] gone ahead to solve the problem of swipe pressure detection. While detection of swipe pressure can open a new dimension of user interaction with natural surfaces, accurate detection of swipe pressure across different materials type can be challenging. This is mainly because the amount of heat transferred to different material types is different even if the swipe pressure is similar. The problem is demonstrated in Fig. 1. Our work proposes to solve this problem by first detecting a

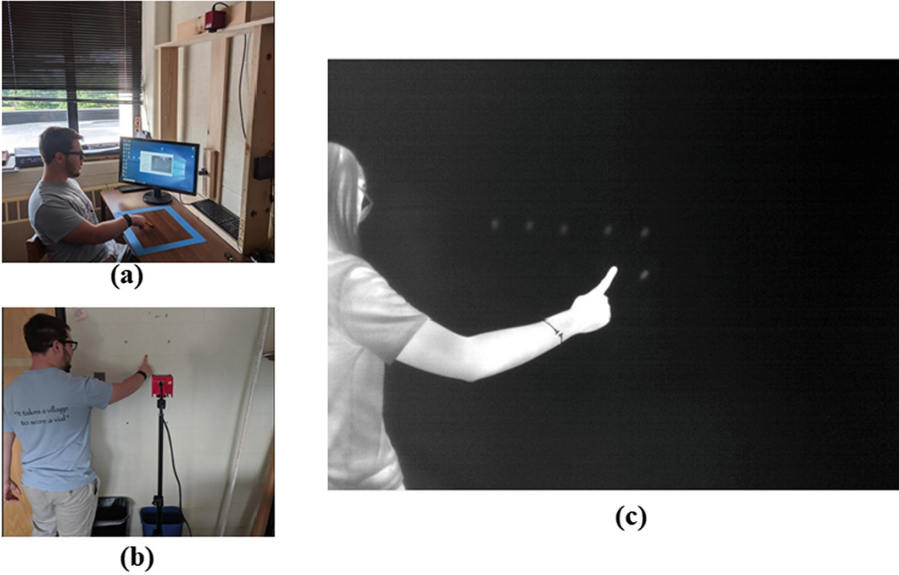


**Fig. 2.** Thermal finger impression data collection setup. (a) Table mounted camera. (b) Tripod mounted camera. (c) Thermal finger impression data on a material surface.

surface material type, and then allowing swipe pressure detection systems to use material-specific classifiers for the task.

There have been a few studies for multi-material detection from thermal images. Gundupalli et al. [9] proposed a material detection system to assist the segregation of recyclables items. However, they require to heat the materials in a dark hot chamber with controlled temperature. Cho et al. [10] use a thermal camera integrated into a mobile phone to capture thermal images of indoor and outdoor materials, and they utilize thermal texture information for material classification. Unlike this method, our material surfaces are smooth and do not display much texture information in the thermal domain. Aujeszky et al. [11] performed material classification using laser excitation step thermography. Bai et al. [12], use a heat lamp to heat up the local environment and capture the thermal signature of the materials. Our method, on the other hand, does not require any specific hardware system, and it can classify materials that otherwise are difficult to identify with texture features.

### 3 Data Collection

All the data is captured using a Sierra Olympic Viento-G thermal camera with a 9 mm lens. The data is recorded at 30 frames per second (fps) rate and stored as 16 bit TIFF images with  $640 \times 480$  pixels resolution. We collected data from 15 users interacting with 7 different materials such as blackboard, polyester fabric,

cotton cloth, concrete, drywall, laminate, and wood. Five different samples for each material, scattered across 8 different rooms of two buildings, are used in this process. The indoor temperature during data collection was between 65° to 70° Fahrenheit. Before the data collection, we made sure that the users' hand temperature is close to normal human body temperature in the range of 95° to 100° Fahrenheit. For each material sample, users are asked to provide 10 thermal finger impressions. As a result, we collected 5250 (7 materials  $\times$  5 samples  $\times$  15 users  $\times$  10 finger impressions) finger impression examples in total for all users on all material samples. For thermal finger impression data, users are asked to touch the material surface for approximately 2s with their index finger. The transferred heat from the finger to the material surface (thermal finger impression) is recorded for 50s to get the diminishing heat pattern. For the entire duration of data recording, the camera setup is arranged in such a way that the camera axis remains normal to the material surface. The data capturing procedure is illustrated in Fig. 2.

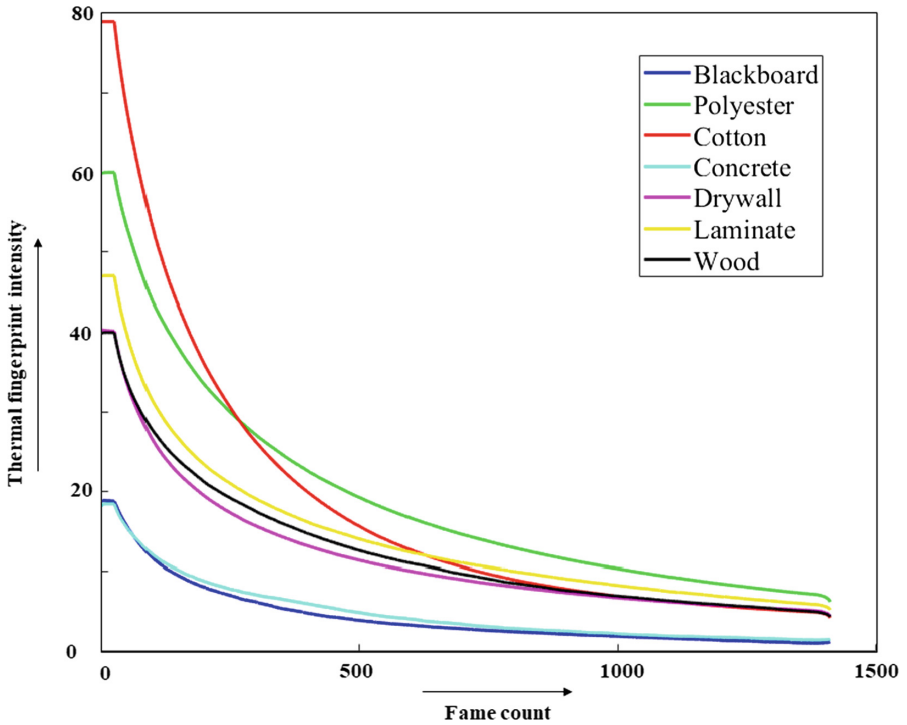


**Fig. 3.** A plot of average time series patterns for 7 different material types. The horizontal axis is corresponding to the frame number relative to the first recorded frame. The vertical axis represents the background-subtracted average pixel value for all thermal finger impression instances of a material type.

## 4 Method

Our method comprises of data pre-processing, feature extraction, and classification. The following sections explain the steps in detail.

### 4.1 Data Pre-processing

We performed mainly two tasks under data pre-processing. Data cleanup, and camera fluctuation correction. In the data cleanup step, we rejected some of the recorded data due to various reasons such as high frame drop rate, thermal finger impression being occluded by the user body part, and a user provides multiple finger impressions in very close proximity that cannot be segregated from each other. We rejected approximately 10% of the data in this process.

We observed different camera fluctuations while analyzing the data. One of the case being the camera automatically performs flat field corrections while recording the data. In this process, it records around 10 frames with high intensity fluctuations which is completely uncorrelated with the thermal signature of the recorded scene. We call these frames as bad frames. Second, after flat field correction occurs, we observe a slight fluctuation in recorded intensity for constant surface temperature. Both of these problems are corrected by observing the average thermal intensity of a small area on recorded frames sequences. This gives us a time series  $T_c = \{t_1, t_2, \dots, t_n\}$ ,  $n$  being the number of frames in the sequence. The area is selected such a way that it does not get occluded by the user at any time point of the recorded duration. Generally, selecting an area from top right corner of the frame works well across all the samples. The bad frame sequence can be easily identified by detecting the frames which produce fluctuations in  $T_c$  greater than a threshold  $Th_{bf} = 200$ . The value of  $Th_{bf}$  is empirically determined. The detected bad frames,  $T_{bf}$ , are ignored in the feature extraction step. To correct the second type of fluctuations, we simply subtracted  $T'_c = \{t'_1, t'_2, \dots, t'_{n'}\}$  from thermal finger impression time series  $F$  explained in Subsect. 4.2. Where,  $T'_c = T_{c-bf} - T^1_{c-bf}$ ,  $T_{c-bf} = \{t^{c-bf}_1, t^{c-bf}_2, \dots, t^{c-bf}_{n'}\} = (T_c - T_{bf})$ ,  $n'$  is number of frames in  $T'_c$  and  $T_{c-bf}$ .  $T^1_{c-bf}$  is a sequence repeating  $t^{c-bf}_1$  for  $n'$  times.

### 4.2 Feature Extraction

Once the image sequences are corrected of camera fluctuations, we extract time series feature vectors from thermal finger impressions. For each of the thermal finger impressions, we manually marked the center pixel and the starting frame where the finger impression is first observed. An  $11 \times 11$  pixels square patch is then selected around the center pixels as a Region of Interest (ROI). We used the background subtraction technique to compute the mean thermal intensity difference caused by the finger impression ROI. For this purpose, we computed the background model  $bg$  as the average of the first 10 frames of a recording sequence. Suppose the frame sequence starting from the first frame marked for the thermal finger impression is  $S = \{s_1, s_2, \dots, s_{1500}\}$ . The length of the sequence is 1500 as

we observed the finger impression for 50 s at 30 fps rate. The time series feature  $F = \{f_1, f_2, f_{1500}\}$  is then computed as  $f_i = \text{mean}(\text{differ}(s_{ROI,i}, bg_{ROI}))$ ,  $i \in [1, 1500]$ . Where  $s_{ROI,i}$  is the ROI on frame  $s_i$ ,  $bg_{ROI}$  is the ROI on the background model. The operation  $\text{differ}(s_{ROI,i}, bg_{ROI})$  performs pixel-wise subtractions of  $bg_{ROI}$  from  $s_{ROI,i}$ . Finally,  $\text{mean}(\cdot)$  computes the average of all pixel-wise differences in  $\text{differ}(s_{ROI,i}, bg_{ROI})$ .

As expected, the extracted time series features mostly follow a non-increasing curve. Figure 3 displays the time series computed by averaging all finger impression time series for each of the 7 material types. As it can be seen, the time series patterns of blackboard and concrete are very similar. The same is applicable for drywall, laminate, and wood. This suggested us to club blackboard and concrete in one cluster and drywall, laminate, and wood in another cluster. Below are the features we considered for the classification framework. Before computing the features, a one-dimensional median filter with window size 51 is used for denoising the time series.

*Raw Time Series:* This is the 1500 dimensional time series  $F$  computed for each of the thermal finger impressions.

*Relative Time Series:* 1500 dimensional time series  $F'$  constructed by computing absolute differences of  $f_1$  and each element of  $F$ . Sometimes, feature vectors of different samples of the same material can show some variance in absolute values. This feature can help to preserve the decay pattern of the time series ignoring the variance of absolute values. We used the 3000-dimensional concatenation of  $F$  and  $F'$  as the feature vector.

*Polynomial Coefficients:* We fitted a polynomial of degree 2 and a polynomial of degree 3 on each of the time series. The 7 polynomial coefficients (3 coefficients of the polynomial of degree 2 followed by 4 coefficients of the polynomial of degree 3) are used as a feature vector.

*Median Samples:* A time series  $F$  is divided into  $k$  equal parts. The median values of each part are computed constructing a  $k$  dimensional feature vector. This helps to ignore local distortion of features due to unexpected noise. Different value of  $k$  is used starting from 10 to 100 with a stride of 10.

*Relative Median Samples:* A  $k$  dimensional median samples vector is computed on  $F'$ , and it is concatenated with the  $k$  dimensional median samples on  $F$ . Therefore, a  $k$  relative median samples feature vector is a  $2 \times k$  dimensional vector.

### 4.3 Classification

We divided our data set into two parts. The first part consists of data from users 1 to 10 and we call it the training set. The second part consists of data from users 11 to 15 and this is called the test set. We used a random forest classifier

implemented in Weka 3.8.3 release [13]. Random forest is a powerful classification model that can naturally handle multiclass classification, robust against nonlinear decision boundaries, and has a relatively low training cost. Therefore, we believe, it would be wise to validate our dataset with a random forest classifier. The training set is used for 10 fold cross validation using each of the features described in Subsect. 4.2. Finally, the best features, i.e. the 3000 dimensional relative times series, and 200 (100 + 100) dimensional relative median samples, are used for classification on the test set. All the experiments are repeated twice, first time for 7 material types and second time for 4 clusters formed by grouping the materials based on their thermal behavior. Cluster 1 is blackboard and concrete, cluster 2 is polyester fabric, cluster 3 is cotton cloth, and class 4 is drywall, laminate, and wood.

## 5 Results

We performed 10 fold cross validation on the training data set. The results of the experiments are reported in Figs. 4 and 5. Compared to the 7 class classification setup, the 4 class setup improved the best detection accuracy by 21.5%. This is mainly because we cluster together the materials with confusing thermal decay patterns into the same classes. As it can be seen, the raw relative time series feature received the best classification accuracy in both 7 class and 4 class classification setups. However, 200-dimensional relative median samples feature also received high detection rates which are very close to the highest accuracy. While it can be computationally expensive to train a classifier with the 3000-dimensional raw relative time series feature, training with the relative median sample feature is comparatively economical. Therefore, it can serve as a balance between classification accuracy and computational expense. Plots in Fig. 5 suggest that increasing  $k$  from 10 to 100 in median sample features and relative median samples features improve the detection rates around 3% for both 7 class and 4 class classification setups.

While the cross-validation on the training set is used only for the selection of the best performing features, the actual validation of our system is performed in a user-independent fashion by training the model using the complete training set and measuring the accuracy on the test set. Please note, our training set contains the data from user 1 to 10, and the test set contains the data from user 11 to 15. The best two performing features, raw relative time series, and 200-dimensional relative median samples are selected for the same. The confusion matrices in Fig. 6 shows the performance of both the features in two different classification scenarios. The confusion matrices in Fig. 6(a), and (b) support our earlier prediction that thermal signatures of materials within classes blackboard-concrete and drywall-laminate-wood are similar. That is the reason that the materials within the same classes are interchangeably getting falsely detected. Irrespective of that, we received around 52% and 75% accuracy in 7 class and 4 class scenarios. Compare to the random guess probability of 14.28% and 25%, this is a significant achievement. Moreover, user samples of the training set and the test

| Material   | Raw     | Raw Rel. | Coeffs. | Med 100 | Rel Med 200 |
|------------|---------|----------|---------|---------|-------------|
| Blackboard | 65.5263 | 66.3158  | 52.6316 | 61.0526 | 65          |
| Polyester  | 74.6512 | 80       | 69.3023 | 75.1163 | 81.1628     |
| Cotton     | 87.7551 | 89.3878  | 87.551  | 88.5714 | 87.7551     |
| Concrete   | 49.7561 | 48.5366  | 47.0732 | 50.2439 | 51.4634     |
| Drywall    | 56.7442 | 56.9767  | 45.3488 | 58.3721 | 59.3023     |
| Laminate   | 36.25   | 40.25    | 30.75   | 38.25   | 38.5        |
| Wood       | 30.8333 | 36.9444  | 28.0556 | 31.6667 | 34.4444     |
| Overall    | 58.76   | 61.1     | 53.07   | 59.07   | 61.03       |

**(a)**

| Material Class | Raw     | Raw Rel. | Coeffs. | Med 100 | Rel Med 200 |
|----------------|---------|----------|---------|---------|-------------|
| 1              | 87.5949 | 88.481   | 82.7848 | 82.0253 | 87.9747     |
| 2              | 69.3023 | 72.093   | 60.6977 | 57.2093 | 72.093      |
| 3              | 85.9184 | 85.9184  | 85.9184 | 81.0204 | 85.5102     |
| 4              | 81.1765 | 81.7647  | 77.0588 | 72.2689 | 81.7647     |
| Overall        | 81.97   | 82.86    | 77.69   | 81.83   | 82.66       |

**(b)**

**Material Class: 1 = Blackboard-Concrete, 2 = Polyester, 3 = Cotton, 4 = Drywall-Laminate-Wood.**

**Fig. 4.** Classification accuracy on the training set is reported (a) for 7 material classes and (b) 4 material classes. Columns 2 to 6 are accuracies for raw time series, relative time series, polynomial coefficients, median samples, and relative median samples features respectively. All numbers are in percentage.

set are completely separated. This strongly suggests that our algorithm is user-independent i.e. given it trained on enough training examples, it can produce good detection accuracy on unknown test data produced by users outside of the subjects in the training set.

## 6 Discussion

In this paper, we proposed a multi-material detection algorithm that can classify commonly available indoor materials into thermally equivalent clusters. To this process, we employ a novel approach where a user has to briefly touch a surface leaving its thermal finger impression on the material. The decaying heat pattern of the finger impression is then analyzed in a machine learning framework to identify the surface material. The work would be valuable especially for the systems that allow users to use the natural surfaces as touch screen interfaces. We demonstrated the capability of our method as we achieved 75% accuracy

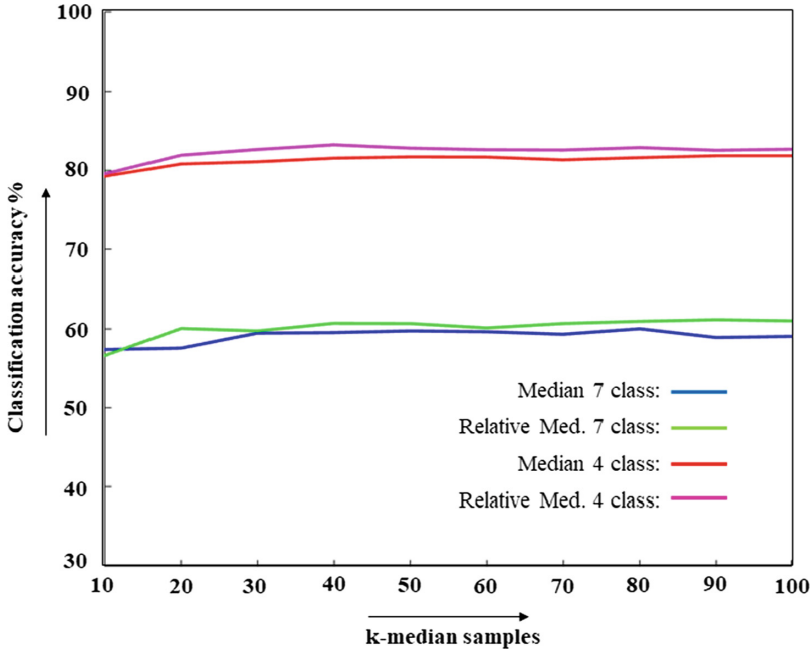


**Fig. 5.** Figure shows the accuracy of the training set on  $k$ -median samples and relative  $k$ -median samples features.  $k$  varies from 10 to 100 with a stride of 10.

in classifying 7 different materials into 4 classes based on the similarity of their thermal behavior. Moreover, we experimentally proved that our algorithm is user-independent. There can be two major reasons behind this. First, our defined task for the thermal finger impression is simple i.e. touching the surface material for two seconds with the index finger. Therefore, the between users' thermal finger impression variations for the same material are less compared to between material variations. Second, the heat decay patterns of a material surface are only dependent on the amount of heat transferred to the surface. Since there is not much variation in thermal finger impressions generated by different users, the decay patterns of the same material type are also not user dependent. This implies that our algorithm does not need to train on new user data to successfully able to predict a material type.

As part of the future work, we want to combine RGB color images with thermal finger impression to further improve our classification accuracy. We believe that the surface texture information in the color domain can assist our classifier with complementary information that would help to improve the prediction capability of our system. Furthermore, we have plans to benchmark our algorithm against different parameter changes such as room temperature and humidity differences, user hand temperature changes, within-class material variances such

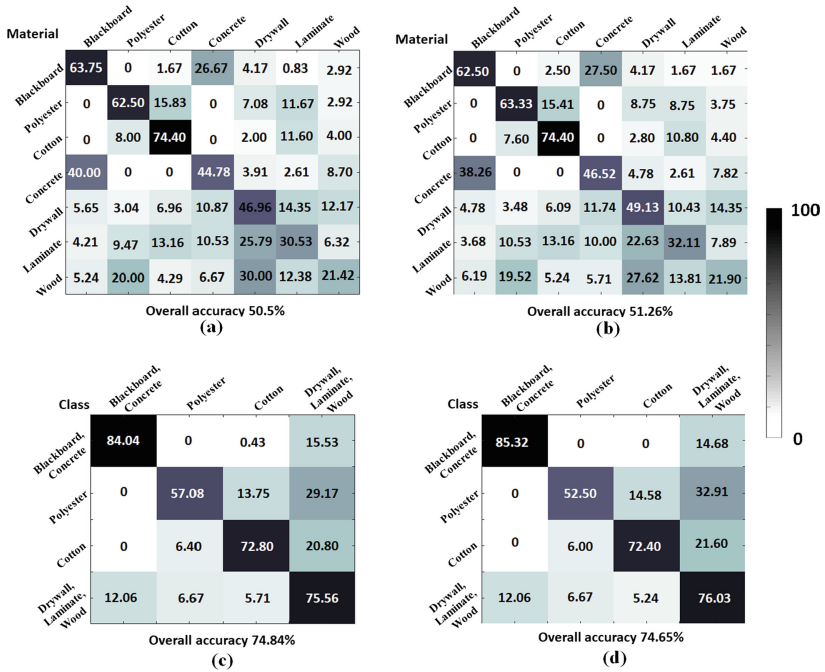


**Fig. 6.** Figure shows the confusion matrices computed on the test set. Accuracy is computed on (a) relative time series and 7 classes, (b) 200 dimensional relative median samples and 7 classes, (c) relative time series and 4 classes, and (d) 200 dimensional relative median samples, and 4 classes. All numbers are in percentage values.

as the same material with different textures. Finally, we would want to use different classification models such as the support vector machine, and deep neural network.

**Acknowledgements.** This work was partially supported by the National Science Foundation (NSF) grant #1730183.

## References

1. Kurz, D.: Thermal touch: thermography-enabled everywhere touch interfaces for mobile augmented reality applications. In: 2014 IEEE International Symposium on Mixed and Augmented Reality, pp. 9–16. IEEE, Munich (2014). <https://doi.org/10.1109/ISMAR.2014.6948403>
2. Wilson, A.D.: Playanywhere: a compact interactive tabletop projection-vision system. In: Proceedings of the 18th Annual ACM Symposium on User Interface Software and Technology, pp. 83–92. ACM, New York (2005)
3. Mistry, P., Maes, P.: Sixthsense: a wearable gestural interface. In: ACM SIGGRAPH ASIA 2009 Sketches, pp. 11. ACM, New York (2009). <https://doi.org/10.1145/1667146.1667160>

4. Oka, K., Sato, Y., Koike, H.: Real-time tracking of multiple fingertips and gesture recognition for augmented desk interface systems. In: Proceedings of the Fifth IEEE International Conference on Automatic Face and Gesture Recognition, pp. 429–434. IEEE Computer Society, Washington, DC (2002). <http://dl.acm.org/citation.cfm?id=874061.875437>
5. Iwai, D., Sato, K.: Heat sensation in image creation with thermal vision. In: Proceedings of the 2005 ACM SIGCHI International Conference on Advances in Computer Entertainment Technology, pp. 213–216. ACM, New York (2005). <https://doi.org/10.1145/1178477.1178510>
6. Saba, E.N., Larson, E.C., Patel, S.N.: Dante vision: in-air and touch gesture sensing for natural surface interaction with combined depth and thermal cameras. In: 2012 IEEE International Conference on Emerging Signal Processing Applications. pp. 167–170, IEEE, Las Vegas (2012). <https://doi.org/10.1109/ESPA.2012.6152472>
7. Larson, E., et al.: HeatWave: thermal imaging for surface user interaction. In: Proceedings of the SIGCHI Conference on Human Factors in Computing Systems, pp. 2565–2574. ACM, New York (2011). <https://doi.org/10.1145/1978942.1979317>
8. Dunn, T., Banerjee, S., Banerjee, N.K.: User-independent detection of swipe pressure using a thermal camera for natural surface interaction. In: 2018 IEEE 20th International Workshop on Multimedia Signal Processing, pp. 1–6. IEEE, Vancouver (2018)
9. Gundupalli, S.P., Hait, S., Thakur, A.: Multi-material classification of dry recyclables from municipal solid waste based on thermal imaging. *J. Waste Manag.* **70**, 13–21 (2017)
10. Cho, Y., Bianchi-Berthouze, N., Marquardt, N., Julier, S.J.: Deep thermal imaging: proximate material type recognition in the wild through deep learning of spatial surface temperature patterns. In: Proceedings of the 2018 CHI Conference on Human Factors in Computing Systems, pp. 1–13. ACM, Montreal (2018). <https://doi.org/10.1145/3173574.3173576>
11. Aujeszky, T., Korres, G., Eid, M.: Thermography-based material classification using machine learning. In: 2017 IEEE International Symposium on Haptic, Audio and Visual Environments and Games, pp. 1–6. IEEE, Abu Dhabi (2017). <https://doi.org/10.1109/HAVE.2017.8240344>
12. Bai, H., Bhattacharjee, T., Chen, H., Kapusta, A., Kemp, C.: Towards Material Classification of Scenes Using Active Thermography. In: 2018 IEEE/RSJ International Conference on Intelligent Robots and Systems, pp. 4262–4269, IEEE, Madrid (2018). <https://doi.org/10.1109/IROS.2018.8594469>
13. Frank, E., Hall, M.A., Witten, I.H.: The WEKA Workbench. Online Appendix for “Data Mining: Practical Machine Learning Tools and Techniques”. Morgan Kaufmann, Burlington (2016)